Lipids in Health and Disease

RESEARCH

Open Access

Deficiency of lysophosphatidic acid receptor 3 decreases erythropoietin production in hypoxic mouse kidneys

Nan Yin[1], Xuyuan Li[1], Di Zhang[1], Mengxia Qu[1], Shengqiang Pei[2], Xi Chen[2], Xiaotian Zhang[1] and Junjie Zhang[1*]

Abstract

Background Lysophosphatidic acid (LPA) is a lipid mediator with diverse biological functions through its receptors on the cell membrane. As one of the six LPA receptors, LPA receptor 3 (LPAR3) is highly expressed in mouse kidneys, but its physiological function in the kidney has been poorly explored.

Methods Wild-type (WT) and *Lpar3*$^{-/-}$ mice were used to investigate the renal physiological function of LPAR3 under hypoxia. The expression levels of LPA receptors in the kidneys of WT mice with or without exposure to hypoxia (8% O_2) were detected by RT–qPCR. RNA sequencing analysis was performed to identify differences in gene expression profiles between the hypoxic kidneys of WT and *Lpar3*$^{-/-}$ mice. The effects of LPAR3 deficiency and treatment with the LPAR1/3 inhibitor Ki16425 or the LPAR3 selective agonist 2S-OMPT on erythropoietin (EPO) production in the kidneys of hypoxic mice were determined by RT–qPCR and ELISAs. The mechanism of LPAR3-mediated regulation of EPO expression was further studied in vivo with mouse models and in vitro with cultured human cells.

Results LPAR3 is the major LPA receptor in mouse kidneys, and its expression is significantly upregulated under hypoxic conditions. RNA sequencing analysis revealed that, compared with WT mice, *Lpar3*$^{-/-}$ mice presented a significant decrease in hypoxia-induced EPO expression in the kidney, together with reduced plasma EPO levels and lower hematocrit and hemoglobin levels. Hypoxic renal EPO expression in WT mice was diminished by the administration of the LPAR1/3 inhibitor Ki16425 and increased by 2S-OMPT, a selective agonist of LPAR3. Hypoxia-induced HIF-2α accumulation in mouse kidneys was impaired by LPAR3 deficiency. Further studies revealed that the PI3K/Akt pathway participated in the regulation of HIF-2α accumulation and EPO expression by LPAR3 under hypoxic conditions.

Conclusions Our study revealed the role of LPAR3 in promoting the HIF-2α–EPO axis in hypoxic mouse kidneys, suggesting that the LPA receptor may serve as a novel potential pharmaceutical target to regulate renal EPO production in hypoxia-related situations, such as chronic kidney disease and altitude disease.

Keywords LPA receptor 3, Erythropoietin, HIF-2α, Hypoxia, Kidney

*Correspondence:
Junjie Zhang
jjzhang@bnu.edu.cn
[1]The Key Laboratory of Cell Proliferation and Regulation Biology, Ministry of Education, Department of Biology, College of Life Sciences, Beijing Normal University, Beijing 100875, China
[2]State Key Laboratory of Cardiovascular Disease, Fuwai Hospital, National Center for Cardiovascular Diseases, Chinese Academy of Medical Sciences and Peking Union Medical College, Beijing, China

Background

As a small biological lipid mediator, LPA functions by binding to a family of six G-protein coupled LPA receptors (LPAR1-6) to activate downstream intracellular signaling pathways and ultimately participates in the regulation of various cellular activities, including proliferation, differentiation, migration, and apoptosis [1, 2]. Among the six LPA receptors, LPAR3, which interacts with $G_{\alpha q/11}$ and $G_{\alpha i/o}$ [3] and belongs to the endothelial cell differentiation gene family with LPAR1 and LPAR2 [4], is widely distributed in mouse and human tissues [5]. Previous studies have revealed the roles of LPAR3 in Hutchinson–Gilford progeria syndrome [6], Huntington's disease [7], cardiac dysfunction [8–10], embryo implantation [11–14], sperm production [15], neuronal network formation [16], dendritic cell migration [17] and circadian rhythm [18]. LPAR3 has been reported to be highly expressed in mouse kidneys [19, 20], and it has been found to play a harmful role in murine renal ischemia–reperfusion injury [20] and to exacerbate diabetic renal damage through podocyte reduction [21]. However, the physiological function of LPAR3 in murine kidneys remains largely unknown. Recently, LPA was shown to promote the development of cancers through the modulation of HIF signaling in in vitro [22–26] and in vivo [27–29] models, which suggests its role in pathological hypoxia. Since the kidney is a well-known hypoxia-sensitive organ, it is worth investigating whether LPA plays a role in the physiological reaction of the kidney to hypoxia through the LPA receptor, especially LPAR3.

Several factors, such as the high energy demand to reabsorb sodium, low density of peritubular capillaries, poor angiogenesis in adult kidneys, and limited renal vascular dilation ability, make the kidney sensitive to hypoxia [30]. When low partial O_2 is sensed in the kidney, hypoxia-inducible factor (HIF) is stabilized in kidney cells due to reduced hydroxylation by prolyl hydroxylases (PHD) and decreased proteasomal degradation mediated by a ubiquitin ligase E3 complex containing von Hippel–Lindau (VHL), and subsequently upregulates many genes at the transcriptional level in response to oxygen deficiency [31]. Erythropoietin (EPO) is the product of the hypoxia-induced *Epo* gene, whose induction is regulated by HIF-2α rather than HIF-1α in mouse kidneys [32, 33]. EPO is produced and secreted by specialized renal interstitial cells, known as renal EPO-producing cells (REPCs) [34], and then moves to the bone marrow to promote the survival, proliferation, and differentiation of erythroid progenitor cells; increase red blood cell abundance; and ultimately improve the oxygen-carrying capacity of the blood [35].

In this study, we explored the physiological function of LPAR3 in mouse kidneys under hypoxia. Transcriptome analysis was performed *via* deep RNA-seq of kidneys from WT and *Lpar3*$^{-/-}$ mice subjected to systemic hypoxia. Among the differentially expressed genes, *Epo*, a classic hypoxia-inducible gene, showed a decrease in expression with LPAR3 deficiency. The effects of LPAR3 on hypoxic renal EPO expression and the potential underlying mechanisms were further studied in mouse models in vivo and in cultured human cells in vitro by using LPAR3-specific siRNAs and drugs. LPAR3 deficiency impaired the accumulation of HIF-2α in hypoxic conditions, possibly through a decrease in PI3K–AKT pathway activation.

Methods

Animal experiments

Lpar3$^{+/-}$ mice with a BALB/c background were kindly provided by Professor Jerold Chun. Male and female *Lpar3*$^{+/-}$ mice were mated to obtain *Lpar3*$^{-/-}$ and littermate control (*Lpar3*$^{+/+}$) mice (Fig. S1A). The primers used for genotyping were as follows: F 5'-TGACAAGCG CATGGACTTTTTC-3', R1 5'- GAAGAAATCCGCAGC AGCTAA-3' and R2 5'-GCACGAGACTAGTGAGACGT GCTAC-3'. The PCR results revealed a larger band for the KO allele (424 bp) and a band for the WT allele (216 bp) (Fig. S1B). The LPAR3 knockout efficiency in different tissues was verified *via* RT–qPCR (Fig. S1C). All the mice were housed under a 12 h:12 h light–dark cycle with free access to food and water. All animal experiments were approved by the Ethics and Animal Welfare Committee, College of Life Sciences, Beijing Normal University.

For continuous hypoxia, 8–10-week-old male mice were placed in a sealed polymethyl methacrylate container, and then, the oxygen content was decreased from 21 to 8% within 30 min by pumping N_2 into the chamber through the flow-through air delivery system. Age- and sex-matched mice exposed to room air were used as normoxia controls. After hypoxia treatment for the indicated times, the mice were immediately anesthetized with 100 mg/kg pentobarbital sodium for blood collection and then sacrificed to remove the kidneys, which were frozen in liquid nitrogen and then kept at -80 ℃ for RNA and protein detection. For plasma collection, blood samples were anticoagulated with EDTA and then centrifuged at 3500 rpm for 10 min at 4 °C.

Ki16425 is a selective antagonist of LPAR1 and LPAR3, and 2S-OMPT is a selective agonist of LPAR3. For Ki16425 or 2 S-OMPT treatment, the mice were pretreated for 30 min with 30 mg/kg Ki16425 (CAS No: 355025-24-0; Selleck, Washington, USA) in 95% corn oil containing 5% dimethyl sulfoxide (DMSO) or 10 mg/kg 2S-OMPT (CAS No: 645408-61-3; Echelon Biosciences, Utah, USA) dissolved in 3% (w/v) fatty acid-free BSA/PBS by intraperitoneal injection and then placed into the low-oxygen chamber. In the control group, an equivalent

amount of corn oil+DMSO or 3% fatty acid-free BSA/PBS was administered.

Blood assessment

The hematocrit and hemoglobin levels in mouse blood were determined by a hematology analyzer (Nihon Kohden, CA, USA). EPO levels in mouse plasma were determined by ELISAs (Cat No: KE10031; Proteintech, IL, USA).

RNA sequencing

The hypoxic kidneys were snap-frozen in liquid nitrogen, and then, RNA extraction, RNA detection, cDNA library construction, and Illumina sequencing were performed by Novogene Bioinformatics Technology Co., Ltd. (Beijing, China). Three independent biological replicates were used. The raw RNA-seq data and processed data (gene count and gene FPKM) were submitted to the GEO repository. The GEO accession number is GSE264135. Differential expression analysis was performed through R *via* the DESeq2 package. Genes with P values < 0.05 and |log2FoldChange| ≥ 0.0 according to DESeq2 were considered differentially expressed. For Gene Ontology (GO) and Kyoto Encyclopedia of Genes and Genomes (KEGG) enrichment analyses, the clusterProfiler R package was used. Gene set enrichment analysis (GSEA) was performed *via* https://www.bioinformatics.com.cn, an online platform for data analysis and visualization [36]. GO terms and KEGG pathways with adjusted P values less than 0.05 were considered significantly enriched.

Cell culture and cell treatment

Hep3B cells (purchased from the China National Infrastructure of Cell Line Resource, Beijing, China) and HK2 cells (purchased from Procell, Wuhan, China) were cultured in MEM (Cat No: PM150410; Procell, Wuhan, China) supplemented with 10% FBS, 100 U/mL penicillin, 0.1 mg/mL streptomycin and 0.25 μg/ml amphotericin B in an incubator with 5% CO_2 at 37 °C.

For hypoxic treatment, the cells were placed in a trigas incubator (Thermo Fisher, Bremen, Germany) maintained at low oxygen tension (1% O_2, 5% CO_2, and 94% N_2). For 2S-OMPT and inhibitor treatment, the cells were serum-starved in serum-free MEM for 24 h. After being pretreated with 30 μM Ki16425 or 10 μM LY294002 (Cat No: HY-10108; MCE, NJ, USA) in serum-free MEM containing 0.05 mg/mL fatty acid-free BSA for 20 min, 2S-OMPT was added to the medium for 1 h, after which the cells were placed in a hypoxic incubator for the indicated time. For MG132 (Cat No: HY-13259; MCE, NJ, USA) treatment, Hep3B cells were transfected with nonspecific siRNA (NC siRNA), LPAR3 siRNA-1 or LPAR3 siRNA-2 for 48 h, and then exposed to 1% O_2 for 12 h with or without MG132 (10 μM). For protein half-life assay, the medium containing Cyclohexamide (CHX, Cat No: GC17198; GLPBIO, CA, USA) was pre-equilibrated in 1% O_2 for 1 h. Hep3B cells transfected with siRNA were exposed to 1% O_2 for 12 h, and then HIF-2α protein levels were determined *via* Western blotting after CHX (100 μM) treatment for the indicated time.

Small interfering RNA transfection

Small interfering RNAs (siRNAs) targeting LPAR3 were synthesized by JTSBIO (Wuhan, China). The sequences of the siRNAs used were as follows: LPAR3 siRNA-1, 5'-GCUAAUGAAGACGGUGAUG-3'; LPAR3 siRNA-2, 5'-CCUGACCAACUUGCUGGUUAUUGCU-3'. For knockdown of *Lpar*3 gene expression, the cells were plated and grown in 6-well plates for 24 h before transfection. Then, 25 pmol of siRNAs was transfected into the cells with RNAi MAX Transfection Reagent (Cat No: 13778030; Thermo Scientific, Massachusetts, USA) according to the manufacturer's suggestion. At 48 h after transfection, the knockdown efficiency was determined *via* RT–qPCR, and the cells were subjected to further treatment.

RNA extraction and quantitative real-time PCR analysis

The total RNA of the frozen kidneys or the cultured cells was extracted *via* MagZol reagent (Cat No: R4801-01; Magen, China). One microgram of RNA isolated from the kidney or cultured cells was reverse transcribed by using anchored oligo dT primers and the Reverse Transcription System (Cat No: A3500, Promega Biotech, WI, USA). cDNA was amplified with the specific primers listed in Table **S**1 *via* real-time quantitative PCR (RT–qPCR) with SYBR Green Master Mix (Cat No: 11202ES03; Yeasen, Shanghai, China) and the QuantStudio Real-Time PCR System (Thermo Scientific, Massachusetts, USA). The expression level of each target gene was calculated *via* the $2^{-\Delta\Delta CT}$ method with normalization to the expression level of β-actin or GAPDH.

Western blotting analysis and ELISAs

The frozen mouse kidneys or cultured cells were lysed in RIPA buffer containing a protease inhibitor cocktail (Cat No: HY-K0010; MCE, NJ, USA) and a phosphatase inhibitor cocktail (Cat No: HY-K0021 and HY-K0022; MCE, NJ, USA). Then, the lysates were ultrasonically crushed (15 s on -15 s off, 4 cycles, 3 times in total, Bioruptor) to release the nuclear protein. The supernatant was collected after high-speed centrifugation at 4 ℃, after which the total protein concentration was quantified *via* the BCA assay (Cat No: 23225; Thermo Scientific, Massachusetts, USA). After SDS–PAGE, the proteins were transferred to PVDF membranes (Millipore, CA, USA). The transferred membranes were blocked with 5% milk in TBST for 60 min at room temperature and then immunoblotted with antibodies against HIF-2α (diluted 1:1000,

Cat No: NB100-122, Novus Biologicals, CO, USA), p-AKT (diluted 1:2000, Cat No: 4060 S, Cell Signaling Technology, Massachusetts, USA), AKT (diluted 1:1000, Cat No: 9272 S, Cell Signaling Technology, Massachusetts, USA), β-actin (diluted 1:2000, Cat No: sc-47778, Santa Cruz, CA, USA), or GAPDH (diluted 1:5000, Cat No: 60004-1-Ig, Proteintech, IL, USA) as indicated overnight at 4 ℃. An HRP-conjugated goat anti-mouse antibody (Cat No: ZB-2301, ZSGB-BIO, Beijing, China) or an HRP-conjugated goat anti-rabbit antibody (Cat No: ZB-2305, ZSGB-BIO, Beijing, China) was used as the secondary antibody to detect chemiluminescence signals (Cat No: WBKLS0500; Millipore, CA, USA). For the ELISA analysis of EPO protein in the supernatant of the culture medium, the Human EPO ELISA Kit (Cat No: E-EL-H3640; Elabscience, Wuhan, China) was used.

Statistical analysis

The data from the animal experiments are presented as the means ± SEMs, and the data from the cell experiments are presented as the means ± SDs. Statistical analysis was performed *via* GraphPad Prism (GraphPad). Unpaired t tests were conducted for comparisons between two groups, with two-way analysis of variance (ANOVA) for multiple groups. Differences were considered statistically significant at $p < 0.05$.

Results

Hypoxia increases LPAR3 expression in mouse kidneys

The expression levels of LPA receptors in the kidneys of wild-type (WT) mice were determined *via* RT–qPCR. LPAR1, LPAR2 and LPAR3 were expressed in the kidneys, whereas LPAR4-6 were barely detected. Notably, LPAR3 is the most abundant LPA receptor in mouse kidneys (Fig. 1A), suggesting that LPAR3 may participate in the physiological roles of the kidney. When WT male mice were placed in a low-oxygen (8% O_2+92% N_2) chamber for 12 h, marked accumulation of HIF-2α was observed in the mouse kidneys (Fig. 1B). Moreover, renal *Lpar3*, along with two other hypoxia-induced genes, *Vegfa* and *Glut1*, was significantly upregulated (Fig. 1C), suggesting that *Lpar3* is a hypoxia-inducible gene in the mouse kidney and may play a role in the hypoxia response.

Hypoxia-induced renal EPO expression is decreased by LPAR3 deficiency

We obtained LPAR3 knockout (*Lpar3*$^{-/-}$) mice from Professor Jerold Chun. LPAR3 expression was completely absent in the kidneys of the *Lpar3*$^{-/-}$ mice (Fig. S1C, Fig. 2A), and no compensatory expression of other LPA receptors was observed (Fig. S2). To determine the physiological function of LPAR3 during mouse renal hypoxia, we placed WT and *Lpar3*$^{-/-}$ male mice in a low-oxygen (8% O_2+92% N_2) chamber for 12 h. Then, the mouse kidneys were collected after hypoxic treatment and subjected to transcriptome analysis *via* deep RNA sequencing (RNA-seq). There were 689 genes downregulated and 526 upregulated (DESeq2 P value ≤ 0.05 and |log2FoldChange| ≥ 0.0) by LPAR3 deficiency in the differential expression analysis. After hypoxia exposure, the expression of the *Epo* gene was significantly lower in the *Lpar3*$^{-/-}$ mouse kidneys than in the WT mouse kidneys (Fig. 2B).

For further elucidation of the effect of LPAR3 deficiency on hypoxic renal EPO expression, WT and *Lpar3*$^{-/-}$ mice were maintained under hypoxic (8% O_2) conditions for 6, 12, and 24 h, and EPO mRNA levels in mouse kidneys were determined at each time point. EPO expression in the kidneys of WT mice increased upon hypoxia exposure, peaked at 12 h, and then decreased. In contrast, EPO expression levels in the kidneys of the *Lpar3*$^{-/-}$ mice markedly decreased at each time point throughout hypoxia exposure (Fig. 2C). The reduction in hypoxic renal EPO expression was also reflected in the plasma EPO levels (Fig. 2D). In addition, the WT mice presented a significant hematocrit response and increased hemoglobin levels after 24 h of continuous hypoxic stress, but the two indicators of *Lpar3*$^{-/-}$ mice lagged significantly behind those of WT mice (Fig. 2E, F).

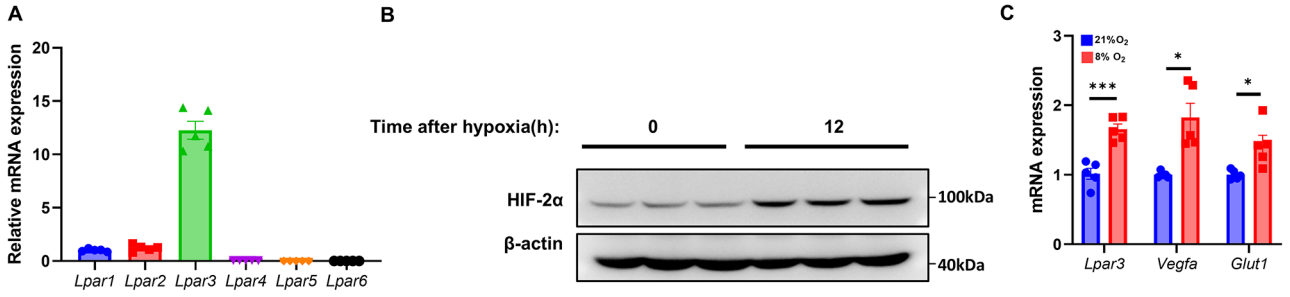

Fig. 1 Hypoxia increases LPAR3 expression in the mouse kidney. **A** The mRNA expression levels of LPA receptors 1–6 were determined in the kidneys of WT mice by RT–qPCR ($n = 5$, mean ± SEM). **B** HIF-2α accumulation after hypoxic exposure was detected in the kidneys of WT mice *via* Western blotting ($n = 3$). **C** Renal *Lpar3*, *Vegfa* and *Glut1* mRNA levels were determined in WT mice with or without hypoxia by RT–qPCR ($n = 5$, mean ± SEM). The *p* value was determined by an unpaired two-tailed Student's *t* test. *$p < 0.5$, ***$p < 0.001$ relative to the normoxia control

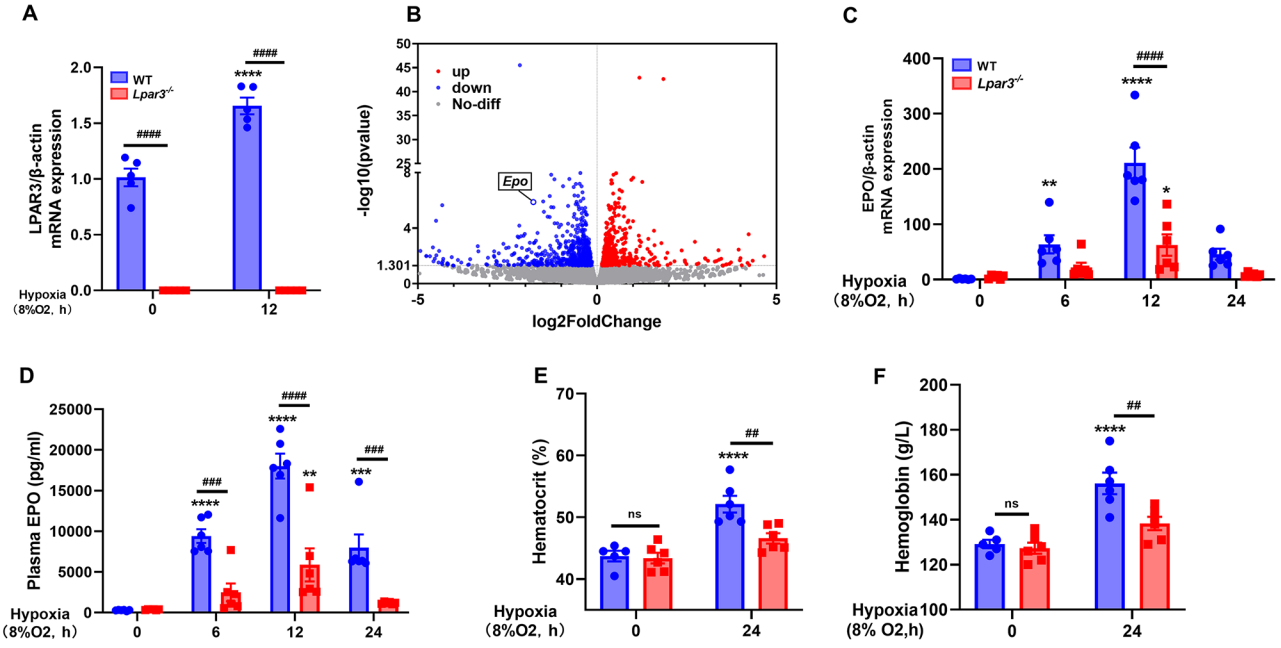

Fig. 2 Hypoxia-induced renal EPO expression is decreased by LPAR3 deficiency in mice. **A** LPAR3 knockout efficiency in the kidneys of *Lpar3*$^{-/-}$ mice was determined *via* RT–qPCR. **B** Volcano plot showing the differentially expressed genes between the WT and *Lpar3*$^{-/-}$ mouse kidneys after hypoxia exposure (8% O_2) for 12 h, and the *Epo* gene is highlighted, $n = 3$. **C–D** Renal EPO mRNA levels **(C)** and plasma EPO levels **(D)** after hypoxia exposure for the indicated times. **E-F** Hematocrit **(E)** and hemoglobin **(F)** levels were determined in the WT and *Lpar3*$^{-/-}$ mice after hypoxia exposure (8% O_2) for 24 h ($n = 5$–6). The *p* value was determined by 2-way analysis of variance (ANOVA) followed by a post hoc test. *$p < 0.05$, **$p < 0.01$, ****$p < 0.0001$ relative to the isogenic normoxia control; ##$p < 0.01$, ###$p < 0.001$, ####$p < 0.0001$ between two genotype groups; mean ± SEM

The impacts of an LPAR3 antagonist and agonist on hypoxic renal EPO expression in mice

The effect of LPAR3 on mouse hypoxic renal EPO expression was further confirmed by the administration of an LPAR3 antagonist and agonist. When WT mice were treated intraperitoneally with the LPAR1/3 antagonist Ki16425 (30 mg/kg) and then placed in a low-oxygen (8% O_2) chamber, both hypoxic renal EPO expression and plasma EPO levels were significantly decreased (Fig. 3A, B). In contrast, preactivation of LPAR3 by its selective agonist 2S-OMPT (10 mg/kg) promoted the response to hypoxia by increasing EPO expression in the kidney and providing more EPO in the blood (Fig. 3C, D). Moreover, the promoting effect of 2 S-OMPT on hypoxic renal EPO expression was completely absent in the kidneys of the *Lpar3*$^{-/-}$ mice (Fig. S3), indicating that 2 S-OMPT functions mainly *via* LPAR3, not *via* other LPA receptors. These results suggest that pharmaceutical targeting of LPAR3 can impact EPO expression in hypoxic mouse kidneys.

LPAR3 deficiency attenuates HIF-2α accumulation in hypoxic mouse kidneys

To reveal the mechanism underlying the regulation of hypoxic renal EPO expression by LPAR3, we assessed the genes that were differentially expressed between the hypoxic kidneys of WT and *Lpar3*$^{-/-}$ mice *via* KEGG enrichment analysis. A total of 47 KEGG pathways were significantly enriched ($P < 0.05$). The hypoxia-inducible factor (HIF) signaling pathway was among the top 20 enriched pathways (Fig. 4A) and tended to be decreased in the hypoxic kidneys of the *Lpar3*$^{-/-}$ mice according to GSEA (Fig. S4A). A heatmap of the downregulated genes enriched in the HIF signaling pathway is shown in Fig. 4B.

Since HIF-2α is the key factor responsible for the induction of mouse renal EPO production during hypoxia stress [32], we propose that insufficient hypoxic EPO production in the kidneys of the *Lpar3*$^{-/-}$ mice may be due to impaired HIF-2α function. As expected, under hypoxic stress, HIF-2α protein levels were significantly increased in the kidneys of the WT mice but not in the kidneys of the *Lpar3*$^{-/-}$ mice (Fig. 4C). Moreover, there was no difference in HIF-2α mRNA levels between the hypoxic kidneys of the WT and *Lpar3*$^{-/-}$ mice, as shown by the RNA-seq data (not shown) and RT−qPCR analysis (Fig. 4D). These results indicate that LPAR3 deficiency attenuates HIF-2α accumulation in hypoxic mouse kidneys.

LPAR3 regulates HIF-2α-EPO signaling in hypoxic cells

Renal EPO-producing cells (REPCs) are special types of peritubular interstitial cells. To date, it has been difficult to obtain primary renal cells in which EPO expression

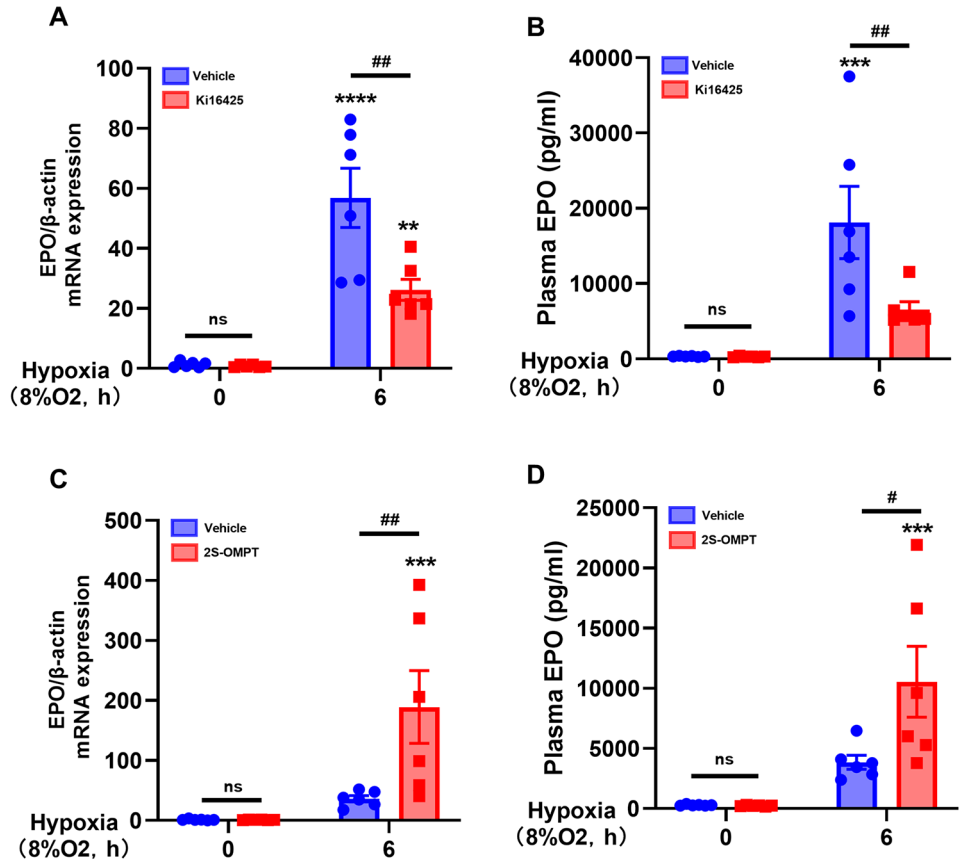

Fig. 3 Effects of an LPAR3 antagonist and agonist on EPO expression in hypoxic mouse kidneys. **A-B** Renal EPO mRNA levels **(A)** and plasma EPO levels **(B)** in the WT mice treated with Ki16425 followed by hypoxia exposure (8% O_2, 6 h). **C-D** Renal EPO mRNA levels **(C)** and plasma EPO levels **(D)** in the WT mice subjected to 2S-OMPT treatment followed by hypoxia exposure (8% O_2, 6 h). $n = 6$ at each time point. The p value was determined by 2-way analysis of variance (ANOVA) followed by a post hoc test. $^{**}p < 0.01$, $^{***}p < 0.001$, $^{****}p < 0.0001$ relative to the isogenic normoxia control; $\#p < 0.05$, $\#\#p < 0.01$ between the two genotype groups; mean ± SEM

can be induced by hypoxia in vitro. Two human hepatoma cell lines, HepG2 and Hep3B, which are capable of producing EPO under hypoxic conditions in vitro, are often used in research on the mechanism of EPO expression regulation [37]. Since HepG2 cells do not express LPAR3, Hep3B cells with LPAR3 expression were used to explore whether LPAR3 could regulate EPO production in hypoxic cells. In the Hep3B cell line, hypoxic EPO expression is regulated mainly by HIF-2α rather than by HIF-1α [38]. First, LPAR3 was knocked down in Hep3B cells with two different LPAR3-specific siRNAs (LPAR3 siRNA-1 and LPAR3 siRNA-2) (Fig. 5A). Hypoxic exposure (1% O_2) significantly induced EPO gene expression in Hep3B cells and increased EPO protein levels in culture medium, which were attenuated by siRNA-mediated LPAR3 knockdown (Fig. 5B, C). In addition, LPAR3 knockdown decreased HIF-2α protein accumulation in Hep3B cells under hypoxic conditions (Fig. 5D), which was consistent with the results obtained in the LPAR3-deficient mouse model. Next, we tested the effect of the LPAR3-specific agonist 2S-OMPT on EPO expression in hypoxic Hep3B cells. Pretreatment with 2S-OMPT significantly increased HIF-2α levels and promoted EPO expression in hypoxic Hep3B cells, whereas these effects were blunted by Ki16425, an LPAR1/3 antagonist (Fig. 5E-G).

In kidney tubular HK2 cells, which cannot produce EPO, LPAR3 knockdown also undermined HIF-2α protein stabilization under hypoxic conditions (Fig. S5A, B). Pharmaceutical targeting of LPAR3 with 2S-OMPT or Ki16425 in HK2 cells had the same effects on HIF-2α accumulation as it did in Hep3B cells (Fig. S5C). Taken together, these results from in vitro hypoxic cells were consistent with those from studies with mouse models, suggesting that the activation of LPAR3 can promote the HIF-2α–EPO axis in the hypoxic response.

LPAR3 promotes the HIF-2α-EPO axis *via* the PI3K-AKT pathway

According to the KEGG analysis, a fraction of the genes that were differentially expressed between the hypoxic kidneys of the WT and *Lpar3*$^{-/-}$ mice were enriched in

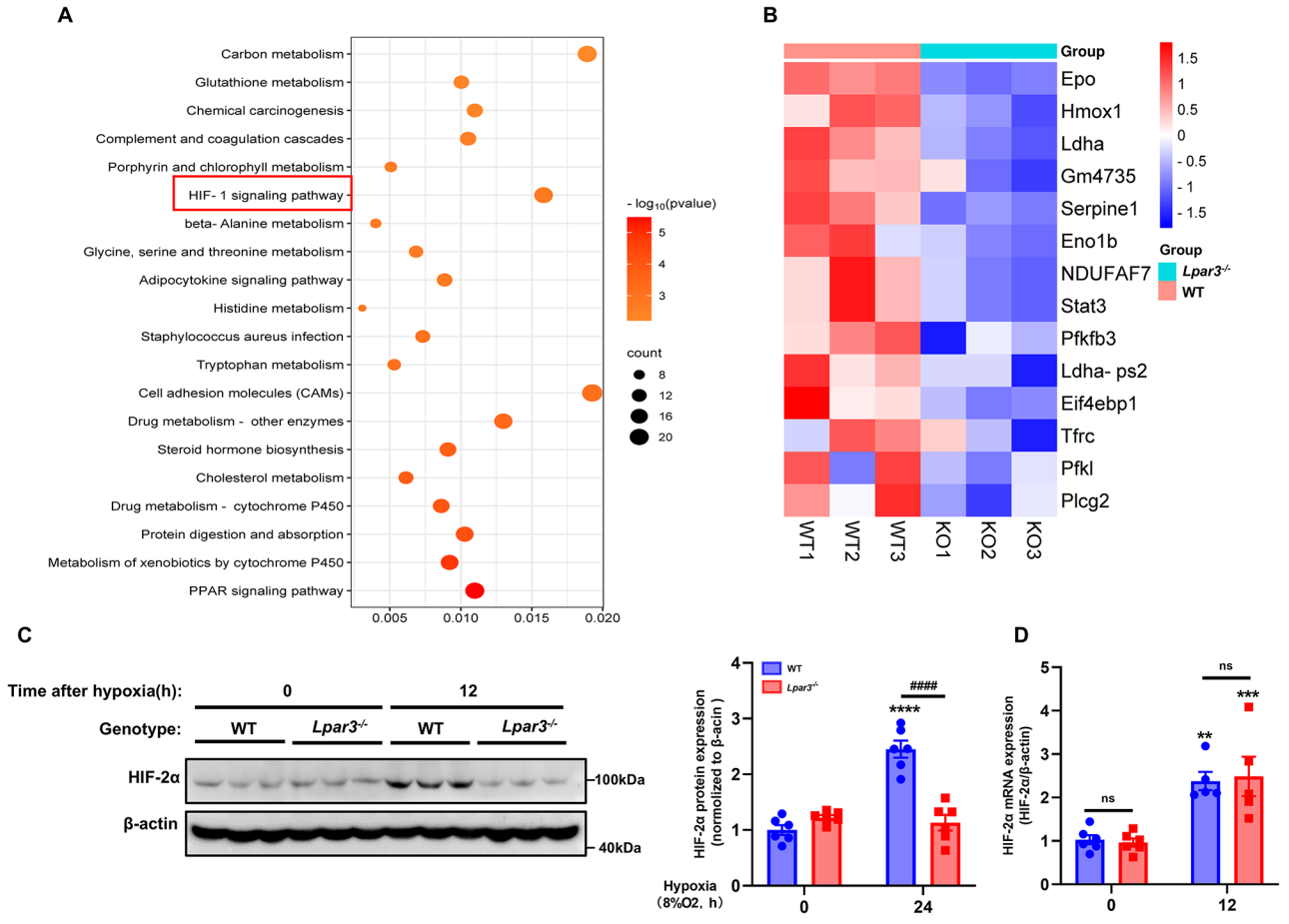

Fig. 4 LPAR3 deficiency attenuates HIF-2α accumulation in hypoxic mouse kidneys. **A** Scatter plot of the top 20 enriched KEGG pathways of all differentially expressed genes between the hypoxic kidneys of the WT and *Lpar3*$^{-/-}$ mice. **B** Heatmap of the enriched genes associated with the HIF-1 signaling pathway downregulated by LPAR3 deficiency. **C** Renal HIF-2α protein levels in the WT and *Lpar3*$^{-/-}$ mice subjected to normoxic or hypoxic conditions were determined *via* Western blotting. **D** HIF-2α mRNA expression was determined by RT–qPCR. $n = 5–6$ per group at each time point. The p value was determined by 2-way analysis of variance (ANOVA) followed by a post hoc test. $^{**}p < 0.01$, $^{***}p < 0.001$, $^{****}p < 0.0001$ relative to the isogenic normoxia control; $\#\#\#\#p < 0.0001$ between two genotype groups; mean ± SEM

the PI3K-Akt pathway, but the difference was not statistically significant ($P=0.068$), and these genes tended to be downregulated in the hypoxic kidneys of the *Lpar3*$^{-/-}$ mice (Fig. S4B). The downregulated genes in this pathway are shown in Fig. 6A. Accordingly, LPAR3 knockout significantly attenuated the hypoxia-induced phosphorylation of Akt in mouse kidneys (Fig. 6B). In Hep3B cells, we also found that hypoxia-induced Akt phosphorylation was attenuated by LPAR3 knockdown (Fig. 6C). Treatment with 2S-OMPT significantly increased Akt phosphorylation and improved HIF-2α accumulation and EPO expression in hypoxic Hep3B cells (Fig. 6D-F). Moreover, the positive effects of 2S-OMPT on Akt phosphorylation and the HIF-2α–EPO axis were eliminated by pretreatment with LY294002, a pan-PI3K inhibitor (Fig. 6D–F). The impacts of LPAR3 on Akt phosphorylation and HIF-2α protein levels were also found in hypoxic kidney tubular HK2 cells (Fig. S6A, B). These data suggest that the PI3K-Akt pathway may function downstream of LPAR3 to participate in the regulation of HIF-2α accumulation and thereby EPO expression under hypoxic conditions.

Discussion

As an important bioactive lipid mediator, LPA exerts diverse biological effects by activating its G protein-coupled receptor (GPCR) on the cell membrane. To date, at least six LPA receptors have been identified. Each subtype of LPA receptor can be coupled with a combination of more than one heterotrimeric G_α subunit ($G_{\alpha q}$, $G_{\alpha i}$, $G_{\alpha 12/13}$, or $G_{\alpha s}$) to modulate downstream signaling pathways [39]. The types and expression levels of LPA receptors vary among different tissues and cell types. In the whole mouse kidney, the mRNA expression levels of LPA receptors followed the pattern LPAR3>>LPAR2>LPAR1>>LPAR4, and LPAR5-6 expression levels were minimal or undetectable (Fig. 1A). Studies have shown that the LPA–LPA receptor signaling pathway is associated with

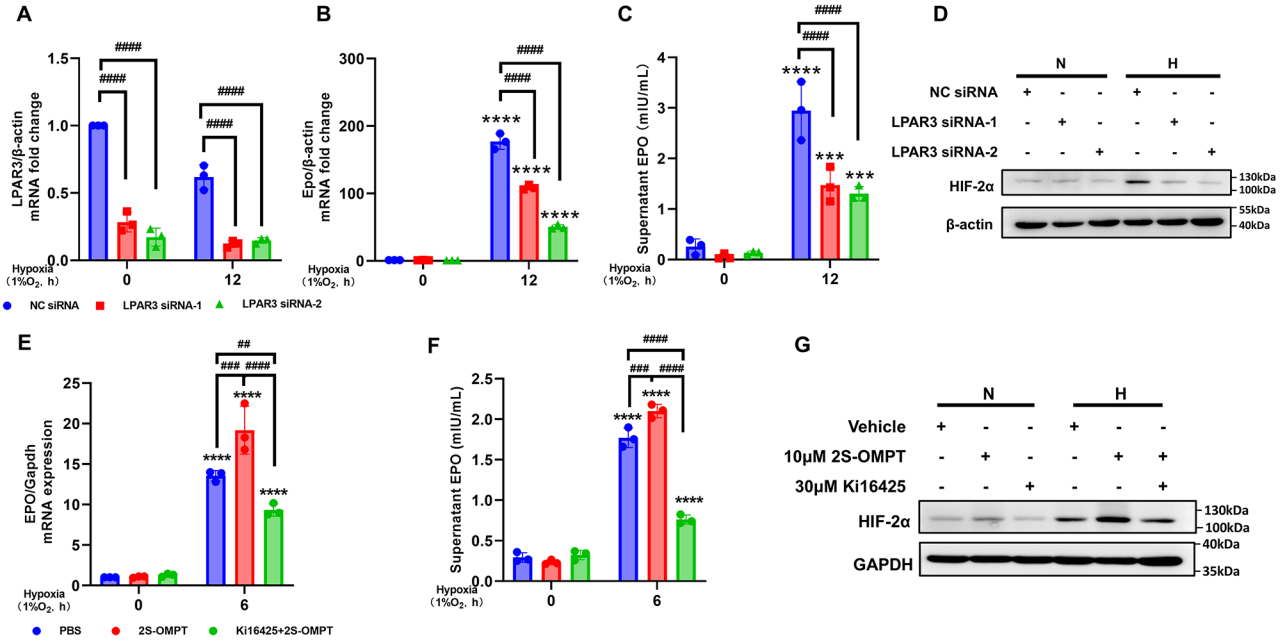

Fig. 5 LPAR3 regulates the HIF-2α–EPO axis in hypoxic Hep3B cells. **A-D** Hep3B cells were transfected with nonspecific siRNA (NC siRNA), LPAR3 siRNA-1 or LPAR3 siRNA-2 for 48 h and then exposed to 1% O_2 for 12 h. LPAR3 mRNA **(A)** and EPO mRNA expression levels **(B)** were determined *via* RT–qPCR, EPO protein levels in culture medium **(C)** were determined *via* ELISAs, and HIF-2α protein levels in Hep3B cells **(D)** were determined *via* Western blotting. **E-G** Hep3B cells were starved in serum-free MEM for 24 h, pretreated in the presence or absence of 30 μM Ki16425 for 20 min, and then challenged with 10 μM 2S-OMPT for 1 h, followed by hypoxia exposure (1% O_2) for 6 h. EPO mRNA expression levels **(E)** were determined *via* RT–qPCR, EPO protein levels in culture medium **(F)** were determined *via* ELISAs, and HIF-2α protein levels in Hep3B cells **(G)** were determined *via* Western blotting. $n = 3$ in each group. The p value was determined by 2-way analysis of variance (ANOVA) followed by a post hoc test. ***$p < 0.001$, ****$p < 0.001$ relative to the normoxia control of the same treatment; ##$p < 0.01$, ###$p < 0.001$, ####$p < 0.0001$, between different siRNA-treated or different drug-treated groups; mean ± SD

various kidney diseases, including acute kidney injury [2, 40, 41], chronic kidney disease [21, 42, 43], renal fibrosis [44–49], and renal cancer [50–52].

As the most abundant LPA receptor subtype in mouse kidneys, LPAR3 has been detected in podocytes of the glomerulus and proximal tubular cells in the renal cortex *via* immunohistochemistry [42]. However, its distribution and expression levels in other specific cell types in the kidney remain unknown. The activation of LPAR3 mainly promotes the recruitment of $G_{\alpha q/11}$ and $G_{\alpha i/o}$ and activates downstream signaling molecules, including phospholipase C, PI3K-AKT, and Ras-MAPK [3]. LPAR3 exacerbates kidney injury after ischemia–reperfusion [20] and causes podocyte injury in diabetic nephropathy [21]. These results were obtained following LPAR3 agonist and LPAR1/3 antagonist treatment. Therefore, research with *Lpar3*$^{-/-}$ mice would be very helpful for improving pharmacology-based studies. In this study, we found that LPAR3 expression was upregulated in mouse kidneys under physiological hypoxia, suggesting that *Lpar3* is a hypoxia-inducible gene. The role of LPAR3 in the hypoxia response was explored in *Lpar3*$^{-/-}$ mice, as were the effects of LPAR3 agonist and antagonist treatment.

Producing and secreting EPO into the bloodstream and later stimulating the production of erythrocytes in the bone marrow is one of the most important functions of the kidney when exposed to hypoxia. In this study, we found that LPAR3 deficiency significantly reduced EPO expression in mouse kidneys and, as a result, diminished erythropoiesis under hypoxia, indicating that LPAR3 plays a role in hypoxic renal EPO induction. Furthermore, pharmaceutical treatment targeting LPAR3 confirmed its impact on mouse hypoxic renal EPO expression. In WT BALB/c mice, treatment with the selective LPAR3 agonist 2S-OMPT improved the response to hypoxia by increasing EPO expression in the kidney. Moreover, in *Lpar3*$^{-/-}$ mice, the stimulatory effect of 2S-OMPT on EPO expression in hypoxic kidneys was completely absent (Fig. S3), suggesting that LPAR3 is the essential target of 2S-OMPT that impacts hypoxic renal EPO expression. In contrast, the administration of the LPAR1/3 antagonist Ki16425 reduced hypoxic renal EPO expression (Fig. 3). The effects of the LPAR3 agonist and antagonist on EPO induction by hypoxia were also observed in Hep3B cells in vitro. In addition, Chiang [53, 54] and Lin [55] reported that, in cord blood-derived human hematopoietic stem cells (hHSCs) and K562 cells, LPAR3 was capable of promoting red blood cell differentiation directly and that injecting mice peritoneally with 2S-OMPT every day for one week resulted in increased erythropoiesis. Overall, LPAR3 may participate in the response to hypoxia in two ways: the promotion of EPO

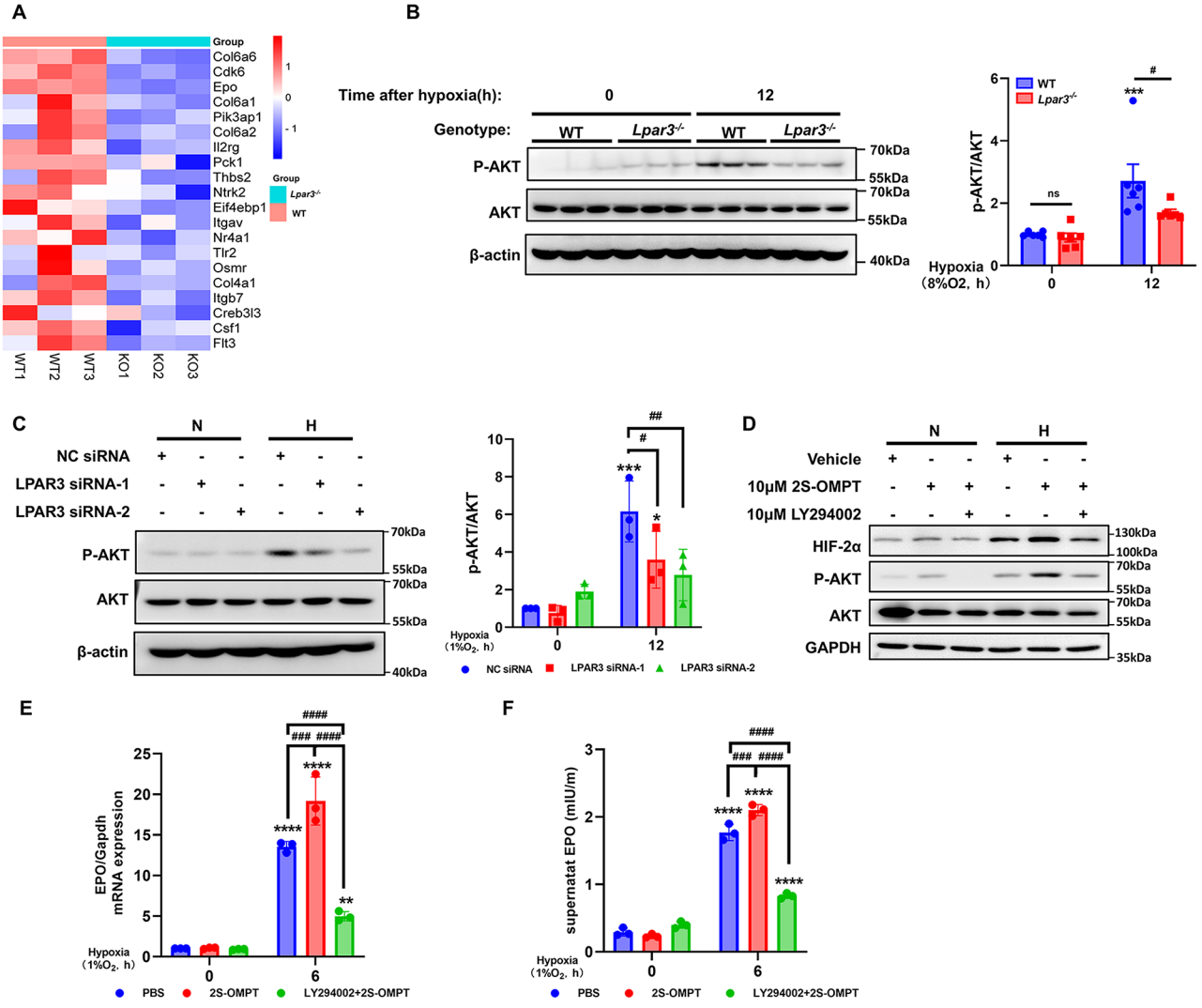

Fig. 6 LPAR3 promotes the HIF-2α–EPO axis *via* the PI3K–AKT pathway. **A** Heatmap of the downregulated genes enriched in the PI3K–Akt signaling pathway in the kidneys of hypoxic mice with LPAR3 deficiency. **B** The total renal AKT and p-AKT levels in the WT and *Lpar3*$^{-/-}$ mice under normoxic or hypoxic conditions (8% O_2) were determined by Western blotting, $n = 6$. The p value was determined by 2-way analysis of variance (ANOVA) followed by a post hoc test. ***$p < 0.001$ compared with the isogenic normoxia control; #$p < 0.05$ between different genotype groups; mean ± SEM. **C** Hep3B cells were transfected with nonspecific siRNA (NC siRNA), LPAR3 siRNA-1 or LPAR3 siRNA-2 for 48 h and then exposed to 1% O_2 for 12 h. Total AKT and phosphorylated AKT (p-AKT) levels were determined *via* Western blotting. **D-F** Hep3B cells were starved in serum-free MEM for 24 h, pretreated with or without LY294002 (10 μM) for 20 min, and then challenged with 2S-OMPT for 1 h, followed by hypoxia exposure (1% O_2) for 6 h. Total AKT, p-AKT, and HIF-2α protein levels were determined by Western blotting **(D)**. The EPO mRNA expression levels **(E)** were determined *via* RT–qPCR, and the EPO protein levels in the culture medium **(F)** were determined *via* ELISAs. The p value was determined by 2-way analysis of variance (ANOVA) followed by a post hoc test. **$p < 0.01$, ****$p < 0.0001$ relative to the normoxia control of the same treatment; ###$p < 0.001$, ####$p < 0.0001$, between different drug-treated groups; mean ± SD

induction in the kidney and the promotion of red cell differentiation in the bone marrow.

EPO is a glycoprotein hormone that promotes erythropoiesis through a specific receptor, EpoR, on the surface of immature red blood cells. The activation of EpoR inhibits cell apoptosis and promotes cell differentiation into mature red blood cells [56]. EPO is induced in the kidney by hypoxia and is secreted into the blood to promote the formation of red blood cells and improve the oxygen-carrying capacity of the blood. This oxygen-sensing mechanism of the kidney plays a key role in regulating erythropoiesis and coping with hypoxia [57]. Studies have shown that EPO expression is strictly regulated by HIF-2α in adult mouse kidneys [32, 33]. HIF-2α protein levels are regulated by tissue oxygen partial pressure and are significantly increased during hypoxia. In this study, we found that LPAR3 deficiency attenuated HIF-2α accumulation under hypoxia in mouse kidneys and that LPAR3 knockdown suppressed the increase in HIF-2α protein levels caused by hypoxia in different cell lines (Hep3B cells and HK2 cells). In addition, treatment with the LPAR3 agonist 2S-OMPT further increased

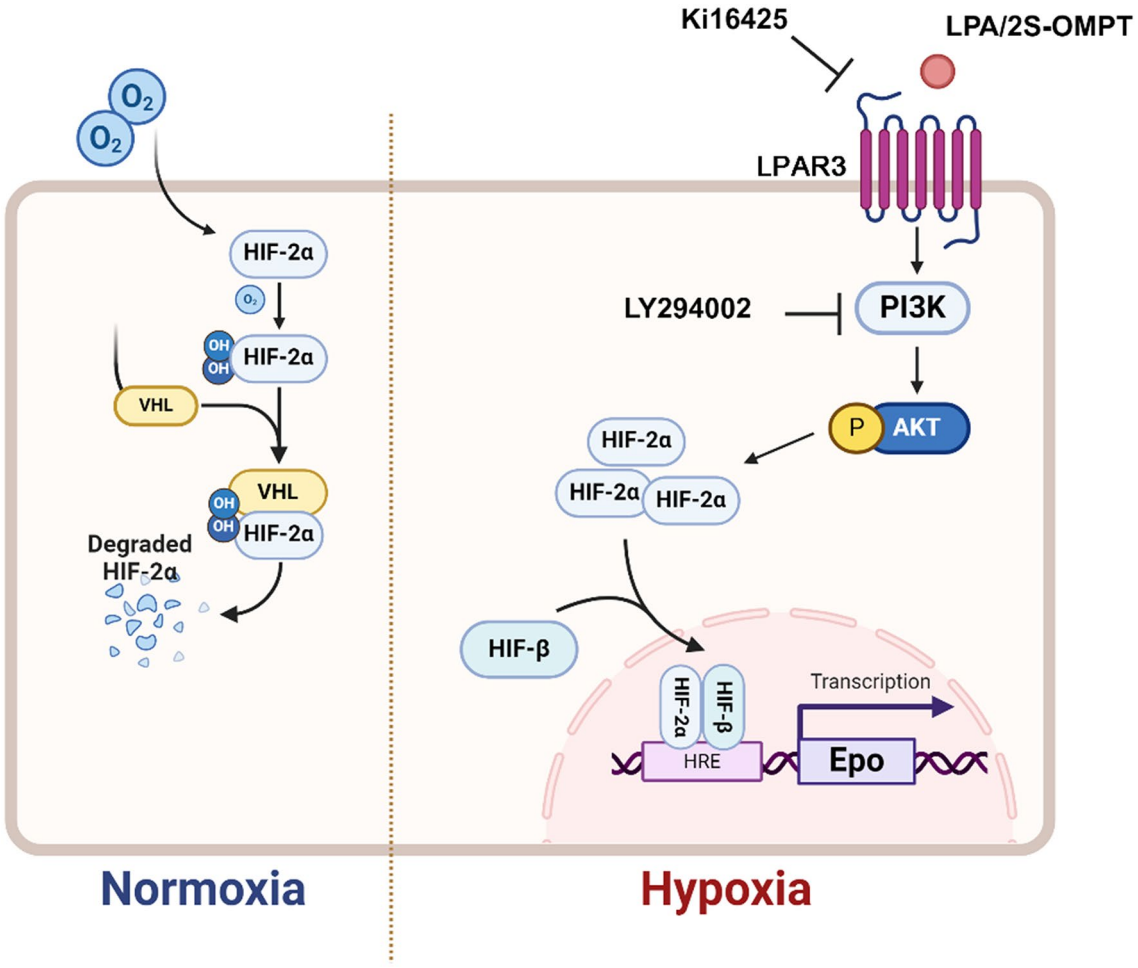

Fig. 7 LPAR3 regulates EPO induction by hypoxia. In hypoxic cells, LPAR3 is activated by LPA or its agonist OMPT, resulting in PI3K-Akt pathway activation, which contributes to the stabilization of HIF-2α. The stabilized HIF-2α subsequently translocates into the nucleus and forms a heterodimer with HIF-β to bind with the HRE (HIF-responsive element) in the *Epo* promoter for transcriptional activation of the *Epo* gene. The induction of EPO by hypoxia is suppressed by treatment with the LPAR1/3 inhibitor Ki16425 or LY294002, a pan-PI3K inhibitor

HIF-2α accumulation and promoted EPO induction in hypoxic Hep3B cells, but these effects were blunted when the agonist was co-administered with the LPAR1/3 antagonist Ki16425.

In this study, it was found that HIF-2α protein levels, but not its mRNA levels, were decreased by LPAR3 deficiency in hypoxic mouse kidneys (Fig. 4C and D) and by LPAR3 knockdown in hypoxic human cells (Fig. 5D, S5B and S7A), indicating that LPAR3 regulates hypoxic HIF-2α expression at the post-transcriptional level. Further research found that the PI3K-AKT pathway downstream of LPAR3 is involved in the regulation of HIF-2α protein levels under hypoxic conditions (Fig. 6). Previous studies have shown that the PI3K-AKT pathway can regulate HIF-α (primarily HIF-1α) at transcription [58], translation [59], and protein stability levels [60–62]. In hypoxic Hep3B cells, we found that the half-life of HIF-2α protein was shortened by LPAR3 knockdown (Fig. S7B), and that the suppression of HIF-2α accumulation by LPAR3 knockdown was blocked by the proteasome inhibitor MG132 (Fig. S7C). These results suggest that LPAR3 may positively regulate HIF-2α stability through suppressing the proteasome-dependent HIF-2α degradation.

LPA can be generated both intra- and extracellularly [63]. Autotaxin (ATX) is responsible for the major production of extracellular LPA from lysophosphatidylcholine (LPC) [64]. Our previous study revealed that hypoxia increase the expression of ATX *via* HIF-2α [26], indicating a direct association between the ATX–LPA axis and hypoxia. Interestingly, renal ATX expression was upregulated, and LPAR3 deficiency led to decreased ATX expression in hypoxic mouse kidneys (Fig. S8), which may have been due to impaired HIF-2α accumulation, suggesting positive feedback regulation between the HIF-2α–ATX–LPA axis and the LPA–LPAR3–HIF-2α axis in hypoxic mouse kidneys. The phospholipase A (PLA)-type enzymes (PLA1 and PLA2) also contribute to

extracellular LPA production through hydrolyzing fatty acid of the phosphatidic acid (PA) [65, 66]. Intracellularly, LPA can be generated from glycerol-3-phosphate by glycerol-3-phosphate acyltransferase (GPAT) [67] and from monoacylglycerol by monoacylglycerol kinase (MAGK) [68]. It was found that hypoxia could increase the mRNA levels of *Gpat3* but not *Pla1a* in mouse kidneys (Fig. S9 A, B). *Pla2g2a* (*PLA2*) mRNA levels were barely detectable in mouse kidneys under normoxia. Renal *Pla2g2a* expression was increased by hypoxia exposure but it was still at a very low level (Fig. S9C). Either under normoxic or hypoxic conditions, LPAR3 deficiency did not significantly affect the renal mRNA levels of *Gpat3*, *Pla2g2a*, and *Pla1a* (Fig. S9). It is still unclear whether the intracellularly produced LPA can cross the plasma membrane to act as the extracellular signaling molecule through LPA receptors.

Insufficient production of EPO may cause anemia in some diseases, such as chronic kidney disease and altitude disease. In our study, pharmaceutically activating LPAR3 *via* its specific agonist 2S-OMPT promoted EPO expression in hypoxic mouse kidneys, representing a novel target for treating anemia in these diseases.

Limitations of this study

The kidney has a complex and unique structure composed of various types of cells. EPO is produced by renal EPO-producing cells (REPCs), which are a special type of peritubular interstitial cell [69]. The number of REPCs increases significantly under hypoxic conditions, but it is difficult to obtain primary renal cells in which EPO expression can be induced by hypoxia in vitro [70]. Hep3B cells are often used in research on the mechanism of EPO expression regulation, in which HIF-2α controls EPO induction during hypoxia [71]. In this study, we confirmed the regulation of HIF-2α accumulation and EPO induction by LPAR3 in hypoxic Hep3B cells but not in primary REPCs. Future studies using genetically modified mice deficient in LPAR3 in REPCs would be helpful to address this issue.

Conclusions

This study provides evidence that LPAR3 contributes to the induction of EPO in mouse kidneys following hypoxia exposure. Hypoxia-induced renal EPO expression was significantly decreased in *Lpar3*$^{-/-}$ mice. In WT mice, treatment with the LPAR3 selective agonist 2 S-OMPT promoted EPO induction in hypoxic kidneys, whereas the administration of the LPAR1/3 antagonist Ki16425 inhibited hypoxic renal EPO expression. The accumulation of HIF-2α, the essential factor for the hypoxic induction of EPO in the kidney, was impaired in *Lpar3*$^{-/-}$ mouse kidneys. The PI3K–AKT pathway activated by LPAR3 participates in the regulation of the HIF-2α–EPO axis in both mouse and cellular hypoxic models (Fig. 7).

Abbreviations

LPA	Lysophosphatidic acid
LPAR3	LPA receptor 3
GPCR	G protein-coupled receptor
HIF-2α	Hypoxia-inducible factor 2 alpha
EPO	Erythropoietin
RNA-seq	RNA sequencing
KEGG	Kyoto Encyclopedia of Genes and Genomes
GO	Gene Ontology

Supplementary Information

The online version contains supplementary material available at https://doi.org/10.1186/s12944-024-02367-8.

Supplementary Material 1: Table S1. RT–qPCR primer sequences. Figure S1. Identification of LPAR3 knockout mice. Figure S2. LPAR3 knockout did not affect the expression of other LPA receptors in mouse kidneys under normoxia or hypoxia. Figure S3. The promoting effect of 2S-OMPT on hypoxic renal EPO expression was absent in *Lpar3*$^{-/-}$ mice. Figure S4. Gene set enrichment analysis. Figure S5. LPAR3 regulates HIF-2α expression in hypoxic HK2 cells. Figure S6. LPAR3 promotes HIF-2α expression *via* the PI3K-AKT pathway in hypoxic HK2 cells. Figure S7. LPAR3 regulates HIF-2α protein stability under hypoxia. Figure S8. LPAR3 deficiency blunted the increase of ATX expression in hypoxic mouse kidneys. Figure S9. The mRNA expression levels of LPA-producing enzymes other than ATX in mouse kidneys under normoxic or hypoxic conditions.

Supplementary Material 2: The images of full WB membranes for Figures 1B, 4C, 5D, S5B, S5C, 5G, 6B, 6C, 6D, S7B and S7C.

Acknowledgements

We thank Professor Jerold Chun (Sanford Burnham Prebys Medical Discovery Institute) for providing the *Lpar3*$^{-/-}$ mice, which were generated by Prof. Chun at the University of California, San Diego (UCSD).

Author contributions

N.Y.: Conceptualization, Formal analysis, Investigation, Methodology, Validation, Visualization, Writing original draft; XY. Li.: Resources; D. Zh.: Resources; MX. Qu.: Resources; SQ. P.: Resources; X. Ch.: Resources, Supervision; XT. Zh.: Formal analysis, Funding acquisition, Methodology, Project administration; JJ. Zh.: Conceptualization, Formal analysis, Funding acquisition, Methodology, Project administration.

Funding

This work was supported by grants from the National Natural Science Foundation of China (Nos. 32171138 and 81972604) and the Natural Science Foundation of Beijing Municipality, China (No. 5222012). This work was also supported by the Open Fund from the Key Laboratory of Cell Proliferation and Regulation Biology, Ministry of Education, China.

Data availability

The data supporting the results of this study are available within the manuscript and its supplemental information.The RNA-seq data have been deposited to the GEO repository with the GEO accession number is GSE264135.

Declarations

Ethical approval

All animal experiments in this study were approved by the Ethics and Animal Welfare Committee, College of Life Sciences, Beijing Normal University. The study complied with the relevant ethical regulations pertaining to animal research, and all laboratory animals were cared for and used according to institutional guidelines.

Consent for publication
All authors have read and agreed with the submission of the manuscript to *Lipids in Health and Disease*.

Competing interests
The authors declare no competing interests.

Received: 28 July 2024 / Accepted: 8 November 2024
Published online: 18 November 2024

References

1. Lee JH, Kim D, Oh YS, Jun H-S. Lysophosphatidic Acid Signaling in Diabetic Nephropathy. Int J Mol Sci 2019, 20(11).
2. de Vries B, Matthijsen RA, van Bijnen AA, Wolfs TG, Buurman WA. Lysophosphatidic acid prevents renal ischemia-reperfusion injury by inhibition of apoptosis and complement activation. Am J Pathol. 2003;163(1):47–56.
3. Anliker B, Chun J. Cell surface receptors in lysophospholipid signaling. Semin Cell Dev Biol. 2004;15(5):457–65.
4. Zhao Y, Hasse S, Zhao C, Bourgoin SG. Targeting the autotaxin - lysophosphatidic acid receptor axis in cardiovascular diseases. Biochem Pharmacol. 2019;164:74–81.
5. Shen Y, Yue F, McCleary DF, Ye Z, Edsall L, Kuan S, Wagner U, Dixon J, Lee L, Lobanenkov VV, et al. A map of the cis-regulatory sequences in the mouse genome. Nature. 2012;488(7409):116–20.
6. Chen W-M, Chiang J-C, Lin Y-C, Lin Y-N, Chuang P-Y, Chang Y-C, Chen C-C, Wu K-Y, Hsieh J-C, Chen S-K, et al. Lysophosphatidic acid receptor LPA3 prevents oxidative stress and cellular senescence in Hutchinson-Gilford progeria syndrome. Aging Cell. 2020;19(1):e13064.
7. Jang M, Choi JH, Chang Y, Lee SJ, Nah S-Y, Cho I-H. Gintonin, a ginseng-derived ingredient, as a novel therapeutic strategy for Huntington's disease: activation of the Nrf2 pathway through lysophosphatidic acid receptors. Brain Behav Immun. 2019;80:146–62.
8. Chen J, Chen Y, Zhu W, Han Y, Han B, Xu R, Deng L, Cai Y, Cong X, Yang Y, et al. Specific LPA receptor subtype mediation of LPA-induced hypertrophy of cardiac myocytes and involvement of akt and NFkappaB signal pathways. J Cell Biochem. 2008;103(6):1718–31.
9. Hilal-Dandan R, Means CK, Gustafsson AB, Morissette MR, Adams JW, Brunton LL, Heller Brown J. Lysophosphatidic acid induces hypertrophy of neonatal cardiac myocytes via activation of Gi and rho. J Mol Cell Cardiol. 2004;36(4):481–93.
10. Yang J, Xu J, Han X, Wang H, Zhang Y, Dong J, Deng Y, Wang J. Lysophosphatidic acid is Associated with Cardiac Dysfunction and Hypertrophy by suppressing Autophagy via the LPA3/AKT/mTOR pathway. Front Physiol. 2018;9:1315.
11. Shah BH, Catt KJ. Roles of LPA3 and COX-2 in implantation. Trends Endocrinol Metab. 2005;16(9):397–9.
12. Ye X, Hama K, Contos JJA, Anliker B, Inoue A, Skinner MK, Suzuki H, Amano T, Kennedy G, Arai H, et al. LPA3-mediated lysophosphatidic acid signalling in embryo implantation and spacing. Nature. 2005;435(7038):104–8.
13. Hama K, Aoki J, Inoue A, Endo T, Amano T, Motoki R, Kanai M, Ye X, Chun J, Matsuki N, et al. Embryo spacing and implantation timing are differentially regulated by LPA3-mediated lysophosphatidic acid signaling in mice. Biol Reprod. 2007;77(6):954–9.
14. Aikawa S, Kano K, Inoue A, Wang J, Saigusa D, Nagamatsu T, Hirota Y, Fujii T, Tsuchiya S, Taketomi Y, et al. Autotaxin-lysophosphatidic acid-LPA3 signaling at the embryo-epithelial boundary controls decidualization pathways. EMBO J. 2017;36(14):2146–60.
15. Ye X, Skinner MK, Kennedy G, Chun J. Age-dependent loss of sperm production in mice via impaired lysophosphatidic acid signaling. Biol Reprod. 2008;79(2):328–36.
16. Furuta D, Yamane M, Tsujiuchi T, Moriyama R, Fukushima N. Lysophosphatidic acid induces neurite branch formation through LPA3. Mol Cell Neurosci. 2012;50(1):21–34.
17. Chan LC, Peters W, Xu Y, Chun J, Farese RV, Cases S. LPA3 receptor mediates chemotaxis of immature murine dendritic cells to unsaturated lysophosphatidic acid (LPA). J Leukoc Biol. 2007;82(5):1193–200.
18. Lin Y-N, Audira G, Malhotra N, Ngoc Anh NT, Siregar P, Lu J-H, Lee H, Hsiao C-D. A novel function of the Lysophosphatidic Acid receptor 3 (LPAR3) gene in zebrafish on modulating anxiety, circadian rhythm locomotor activity, and short-term memory. Int J Mol Sci 2020, 21(8).
19. Contos JJ, Chun J. The mouse lp(A3)/Edg7 lysophosphatidic acid receptor gene: genomic structure, chromosomal localization, and expression pattern. Gene. 2001;267(2):243–53.
20. Okusa MD, Ye H, Huang L, Sigismund L, Macdonald T, Lynch KR. Selective blockade of lysophosphatidic acid LPA3 receptors reduces murine renal ischemia-reperfusion injury. Am J Physiol Ren Physiol. 2003;285(3):F565–74.
21. Zhang M-Z, Wang X, Yang H, Fogo AB, Murphy BJ, Kaltenbach R, Cheng P, Zinker B, Harris RC. Lysophosphatidic acid receptor antagonism protects against Diabetic Nephropathy in a type 2 Diabetic Model. J Am Soc Nephrol. 2017;28(11):3300–11.
22. Park SY, Jeong KJ, Lee J, Yoon DS, Choi WS, Kim YK, Han JW, Kim YM, Kim BK, Lee HY. Hypoxia enhances LPA-induced HIF-1α and VEGF expression: their inhibition by resveratrol. Cancer Lett. 2007;258(1):63–9.
23. Lee J, Park SY, Lee EK, Park CG, Chung HC, Rha SY, Kim YK, Bae G-U, Kim BK, Han J-W, et al. Activation of hypoxia-inducible factor-1alpha is necessary for lysophosphatidic acid-induced vascular endothelial growth factor expression. Clin Cancer Res. 2006;12(21):6351–8.
24. Yang K, Zheng D, Deng X, Bai L, Xu Y, Cong Y-S. Lysophosphatidic acid activates telomerase in ovarian cancer cells through hypoxia-inducible factor-1alpha and the PI3K pathway. J Cell Biochem. 2008;105(5):1194–201.
25. Song Y, Wu J, Oyesanya RA, Lee Z, Mukherjee A, Fang X. Sp-1 and c-Myc mediate lysophosphatidic acid-induced expression of vascular endothelial growth factor in ovarian cancer cells via a hypoxia-inducible factor-1-independent mechanism. Clin Cancer Res. 2009;15(2):492–501.
26. Qu M, Long Y, Wang Y, Yin N, Zhang X, Zhang J. Hypoxia increases ATX expression by Histone Crotonylation in a HIF-2α-Dependent manner. Int J Mol Sci 2023, 24(8).
27. Ha JH, Radhakrishnan R, Jayaraman M, Yan M, Ward JD, Fung K-M, Moxley K, Sood AK, Isidoro C, Mukherjee P, et al. LPA induces metabolic reprogramming in Ovarian Cancer via a pseudohypoxic response. Cancer Res. 2018;78(8):1923–34.
28. Kim K-S, Sengupta S, Berk M, Kwak Y-G, Escobar PF, Belinson J, Mok SC, Xu Y. Hypoxia enhances lysophosphatidic acid responsiveness in ovarian cancer cells and lysophosphatidic acid induces ovarian tumor metastasis in vivo. Cancer Res. 2006;66(16):7983–90.
29. Li M, Xiao D, Zhang J, Qu H, Yang Y, Yan Y, Liu X, Wang J, Liu L, Wang J, et al. Expression of LPA2 is associated with poor prognosis in human breast cancer and regulates HIF-1α expression and breast cancer cell growth. Oncol Rep. 2016;36(6):3479–87.
30. Evans RG, Smith DW, Lee CJ, Ngo JP, Gardiner BS. What makes the kidney susceptible to Hypoxia? *Anatomical record (Hoboken, NJ: 2007)* 2020, 303(10):2544–52.
31. Taylor CT, Scholz CC. The effect of HIF on metabolism and immunity. Nat Rev Nephrol. 2022;18(9):573–87.
32. Scortegagna M, Ding K, Zhang Q, Oktay Y, Bennett MJ, Bennett M, Shelton JM, Richardson JA, Moe O, Garcia JA. HIF-2alpha regulates murine hematopoietic development in an erythropoietin-dependent manner. Blood. 2005;105(8):3133–40.
33. Haase VH. Regulation of erythropoiesis by hypoxia-inducible factors. Blood Rev. 2013;27(1):41–53.
34. Shih HM, Wu CJ, Lin SL. Physiology and pathophysiology of renal erythropoietin-producing cells. J Formos Med Association = Taiwan Yi Zhi. 2018;117(11):955–63.
35. Elliott S, Sinclair AM. The effect of erythropoietin on normal and neoplastic cells. Biologics. 2012;6:163–89.
36. Tang D, Chen M, Huang X, Zhang G, Zeng L, Zhang G, Wu S, Wang Y. SRplot: a free online platform for data visualization and graphing. PLoS ONE. 2023;18(11):e0294236.
37. Goldberg MA, Glass GA, Cunningham JM, Bunn HF. The regulated expression of erythropoietin by two human hepatoma cell lines. Proc Natl Acad Sci USA. 1987;84(22):7972–6.
38. Chen R, Xu M, Hogg RT, Li J, Little B, Gerard RD, Garcia JA. The acetylase/deacetylase couple CREB-binding protein/Sirtuin 1 controls hypoxia-inducible factor 2 signaling. J Biol Chem. 2012;287(36):30800–11.
39. Nan Y, Jun-Jie Z. Autotaxin-LPA Axis in obesity and obesity-related diseases. PROGRESS Biochem Biophys. 2021;48(7):768–78.
40. Gao J, Zhang D, Yang X, Zhang Y, Li P, Su X. Lysophosphatidic acid and Iovastatin might protect kidney in renal I/R injury by downregulating MCP-1 in rat. Ren Fail. 2011;33(8):805–10.
41. Okusa MD, Ye H, Huang L, Sigismund L, Macdonald T, Lynch KR. Selective blockade of lysophosphatidic acid LPA3 receptors reduces murine renal ischemia-reperfusion injury. Am J Physiol Ren Physiol. 2003;285(3):F565–574.

42. Li HY, Oh YS, Choi JW, Jung JY, Jun HS. Blocking lysophosphatidic acid receptor 1 signaling inhibits diabetic nephropathy in db/db mice. Kidney Int. 2017;91(6):1362–73.
43. Lee JH, Sarker MK, Choi H, Shin D, Kim D, Jun HS. Lysophosphatidic acid receptor 1 inhibitor, AM095, attenuates diabetic nephropathy in mice by downregulation of TLR4/NF-κB signaling and NADPH oxidase. Biochim et Biophys acta Mol Basis Disease. 2019;1865(6):1332–40.
44. Hirata T, Smith SV, Takahashi T, Miyata N, Roman RJ. Increased levels of renal lysophosphatidic acid in Rodent models with Renal Disease. J Pharmacol Exp Ther. 2021;376(2):240–9.
45. Cortinovis M, Aiello S, Mister M, Conde-Knape K, Noris M, Novelli R, Solini S, Rodriguez Ordonez PY, Benigni A, Remuzzi G. Autotaxin inhibitor protects from Chronic Allograft Injury in rat kidney allotransplantation. Nephron. 2020;144(1):38–48.
46. Mirzoyan K, Baïotto A, Dupuy A, Marsal D, Denis C, Vinel C, Sicard P, Bertrand-Michel J, Bascands JL, Schanstra JP, et al. Increased urinary lysophosphatidic acid in mouse with subtotal nephrectomy: potential involvement in chronic kidney disease. J Physiol Biochem. 2016;72(4):803–12.
47. Lahaye DH, Walboomers F, Peters PH, Theuvenet AP, Van Zoelen EJ. Phenotypic transformation of normal rat kidney fibroblasts by endothelin-1. Different mode of action from lysophosphatidic acid, bradykinin, and prostaglandin f2alpha. Biochim Biophys Acta. 1999;1449(2):107–18.
48. Zuehlke J, Ebenau A, Krueger B, Goppelt-Struebe M. Vectorial secretion of CTGF as a cell-type specific response to LPA and TGF-β in human tubular epithelial cells. Cell Communication Signaling: CCS. 2012;10(1):25.
49. Pradère JP, Klein J, Grès S, Guigné C, Neau E, Valet P, Calise D, Chun J, Bascands JL, Saulnier-Blache JS, et al. LPA1 receptor activation promotes renal interstitial fibrosis. J Am Soc Nephrol. 2007;18(12):3110–8.
50. Su SC, Hu X, Kenney PA, Merrill MM, Babaian KN, Zhang XY, Maity T, Yang SF, Lin X, Wood CG. Autotaxin-lysophosphatidic acid signaling axis mediates tumorigenesis and development of acquired resistance to sunitinib in renal cell carcinoma. Clin Cancer Res. 2013;19(23):6461–72.
51. Chhabra R, Nanjundan M. Lysophosphatidic acid reverses Temsirolimus-induced changes in lipid droplets and mitochondrial networks in renal cancer cells. PLoS ONE. 2020;15(6):e0233887.
52. Sun K, Chen RX, Li JZ, Luo ZX. LPAR2 correlated with different prognosis and immune cell infiltration in head and neck squamous cell carcinoma and kidney renal clear cell carcinoma. Hereditas. 2022;159(1):16.
53. Chiang C-L, Chen S-SA, Lee SJ, Tsao K-C, Chu P-L, Wen C-H, Hwang S-M, Yao C-L, Lee H. Lysophosphatidic acid induces erythropoiesis through activating lysophosphatidic acid receptor 3. Stem Cells. 2011;29(11):1763–73.
54. Chiang J-C, Chen W-M, Lin K-H, Hsia K, Ho Y-H, Lin Y-C, Shen T-L, Lu J-H, Chen S-K, Yao C-L, et al. Lysophosphatidic acid receptors 2 and 3 regulate erythropoiesis at different hematopoietic stages. Biochim Biophys Acta Mol Cell Biol Lipids. 2021;1866(1):158818.
55. Lin K-H, Ho Y-H, Chiang J-C, Li M-W, Lin S-H, Chen W-M, Chiang C-L, Lin Y-N, Yang Y-J, Chen C-N et al. Pharmacological activation of lysophosphatidic acid receptors regulates erythropoiesis. Sci Rep 2016, 6(1).
56. Testa U. Apoptotic mechanisms in the control of erythropoiesis. Leukemia. 2004;18(7):1176–99.
57. Mole DR, Ratcliffe PJ. Cellular oxygen sensing in health and disease. Pediatr Nephrol. 2008;23(5):681–94.
58. Mohlin S, Hamidian A, von Stedingk K, Bridges E, Wigerup C, Bexell D, Påhlman S. PI3K-mTORC2 but not PI3K-mTORC1 regulates transcription of HIF2A/EPAS1 and vascularization in neuroblastoma. Cancer Res. 2015;75(21):4617–28.
59. Albadari N, Deng S, Li W. The transcriptional factors HIF-1 and HIF-2 and their novel inhibitors in cancer therapy. Expert Opin Drug Discov. 2019;14(7):667–82.
60. Ravi R, Mookerjee B, Bhujwalla ZM, Sutter CH, Artemov D, Zeng Q, Dillehay LE, Madan A, Semenza GL, Bedi A. Regulation of tumor angiogenesis by p53-induced degradation of hypoxia-inducible factor 1alpha. Genes Dev. 2000;14(1):34–44.
61. Joshi S, Singh AR, Durden DL. MDM2 regulates hypoxic hypoxia-inducible factor 1α stability in an E3 ligase, proteasome, and PTEN-phosphatidylinositol 3-kinase-AKT-dependent manner. J Biol Chem. 2014;289(33):22785–97.
62. Zhou J, Schmid T, Frank R, Brüne B. PI3K/Akt is required for heat shock proteins to protect hypoxia-inducible factor 1alpha from pVHL-independent degradation. J Biol Chem. 2004;279(14):13506–13.
63. van Meer G, Voelker DR, Feigenson GW. Membrane lipids: where they are and how they behave. Nat Rev Mol Cell Biol. 2008;9(2):112–24.
64. Inoue M, Ma L, Aoki J, Chun J, Ueda H. Autotaxin, a synthetic enzyme of lysophosphatidic acid (LPA), mediates the induction of nerve-injured neuropathic pain. Mol Pain. 2008;4:6.
65. Inoue A, Arima N, Ishiguro J, Prestwich GD, Arai H, Aoki J. LPA-producing enzyme PA-PLA$_1$α regulates hair follicle development by modulating EGFR signalling. Embo j. 2011;30(20):4248–60.
66. Eder AM, Sasagawa T, Mao M, Aoki J, Mills GB. Constitutive and lysophosphatidic acid (LPA)-induced LPA production: role of phospholipase D and phospholipase A2. Clin Cancer Res. 2000;6(6):2482–91.
67. Yamashita A, Hayashi Y, Matsumoto N, Nemoto-Sasaki Y, Oka S, Tanikawa T, Sugiura T. Glycerophosphate/Acylglycerophosphate acyltransferases. Biology. 2014;3(4):801–30.
68. Pagès C, Simon MF, Valet P, Saulnier-Blache JS. Lysophosphatidic acid synthesis and release. Prostaglandins Other Lipid Mediat. 2001;64(1–4):1–10.
69. Bachmann S, Le Hir M, Eckardt KU. Co-localization of erythropoietin mRNA and ecto-5′-nucleotidase immunoreactivity in peritubular cells of rat renal cortex indicates that fibroblasts produce erythropoietin. J Histochem Cytochem. 1993;41(3):335–41.
70. Souma T, Suzuki N, Yamamoto M. Renal erythropoietin-producing cells in health and disease. Front Physiol. 2015;6:167.
71. Tojo Y, Sekine H, Hirano I, Pan X, Souma T, Tsujita T, Kawaguchi S, Takeda N, Takeda K, Fong GH, et al. Hypoxia Signaling Cascade for Erythropoietin Production in Hepatocytes. Mol Cell Biol. 2015;35(15):2658–72.

Publisher's note